Separate determination of diffraction dissociation and absorption contribution to the breakup cross-section of halo nucleus ^{11}Be

F. Negoita, C. Borcea, F. Carstoiu, M. Lewitowicz, M.G. Saint-Laurent, R. Anne, Z. Dlouhy, A. Fomitchev, S. Grévy, D. Guillemaud-Mueller, et al.

GANIL

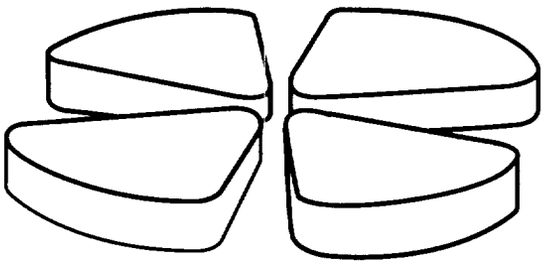

Separate Determination of Diffraction Dissociation and Absorption Contribution to the Breakup Cross Section of Halo Nucleus ^{11}Be

F. Negoita[a,b], C. Borcea[a,b], F. Carstoiu[a,b], M. Lewitowicz[a], M.G. Saint-Laurent[a], R. Anne[a], Z. Dlouhy[c], A. Fomitchev[d], S. Grevy[e], D. Guillemaud-Mueller[e], S. Lukyanov[d], A.C. Mueller[e], F. Pougheon[e], Yu. Penionzhkevich[d], N. Skobelev[d] and O. Sorlin[e]

[a] *GANIL(IN2P3/CNRS,DSM/CEA), BP 5027, 14076 Caen Cedex 5, France;* [b] *IAP, P.O. Box MG-6, 76900 Bucharest-Magurele, Romania;* [c] *NPI, 25068 Rez, Czech Republic;* [d] *FLNR, JINR, 141980 Dubna, Moscow region, Russia;* [e] *IPN, CNRS-IN2P3, 91406 Orsay Cedex, France*

GANIL P 97 23

Separate Determination of Diffraction Dissociation and Absorption Contribution to the Breakup Cross Section of Halo Nucleus ^{11}Be

F. Negoita [a,b], C. Borcea [a,b], F. Carstoiu [a,b], M. Lewitowicz [a], M.G. Saint-Laurent [a] R. Anne [a], Z. Dlouhy [d], A. Fomitchev [e], S. Grevy [c], D. Guillemaud-Mueller [c], S. Lukyanov [e], A.C. Mueller [c], F. Pougheon [c], Yu. Penionzhkevich [e], N. Skobelev [e] and O. Sorlin [c]

[a] *GANIL(IN2P3/CNRS,DSM/CEA), BP 5027, 14076 Caen Cedex 5, France*

[b] *IAP, P.O. Box MG-6, 76900 Bucharest-Magurele, Rumania*

[c] *IPN, CNRS-IN2P3, 91406 Orsay Cedex, France*

[d] *NPI, 25068 Rez, Czech Republic*

[e] *FLNR, JINR, 141980 Dubna, Moscow region, Russia*

Abstract

An integral method has been applied to obtain the 1 and 2n breakup cross sections for ^{11}Be on Si in a wide energy range. The contribution to the breakup of the two mechanisms: stripping and diffraction has been determined and compared to the model predictions. The method allowed for the measurement of parallel momentum distribution of the heavy breakup product in both cases of the mentioned mechanisms. Charge changing cross sections for ^{10,11}Be complemented the measurements.

The discovery of halo nuclei opened a new opportunity to study nuclear matter at low densities. Due to the weak binding energy of halo nucleon, they can be found at relatively large distances from the core and they can also be easily shaken off at the passage through a nuclear and/or Coulomb field. This breakup mechanism is called diffraction/Coulomb dissociation. Another possible breakup mechanism is that in which, for a halo nucleus moving onto a target at rather large impact parameters (e.g. 6-7 fm), the loosely bound halo nucleon(s) can be removed by the target nucleus, while the core-target nuclear interaction is not very important at these distances. This mechanism is called absorption or stripping. Though calculated in different theoretical approaches, these two components were not known experimentally, only their sum (total breakup cross section) being measured.

In the following, a method will be presented that allowed a separate determination of the two contributions to the breakup cross section of ^{11}Be, a known one neutron halo nucleus, on silicon. In the same experiment were also determined: the energy dependence of the mentioned contributions, parallel momentum distributions of ^{10}Be resulting from breakup for diffraction and for stripping at several energies, two neutron removal cross section and charge changing cross sections for ^{10,11}Be. All these data, taken in a single experiment, offer important new information about the reaction mechanism and put severe constraints on the theoretical calculations.

A ^{11}Be secondary beam of 43 MeV/nucleon was produced at GANIL by fragmenting an ^{18}O beam of 70 MeV/nucleon onto a Be target. The fragmentation products were separated and formed by the doubly achromatic spectrometer LISE. About 1000 ^{11}Be per second hit a stack of 17 silicon detectors that served as target, energy degrader and detecting/identifying media for the reaction products. All incident ^{11}Be ions have been stopped in the telescope, most of them in the last detector. The ^{10}Be ions resulting from breakup had a shorter path than the incident particles. The thicknesses of the detectors (300, 4×1000, 500, 150, 500, 300, 3×150, 3×40, 24 and 1000μm), were chosen such as to provide a good separation between beryllium isotopes which required that ^{10}Be produced by a reaction in a given detector should go through at least two other successive detectors before being stopped. Behind the telescope, an array of 32 neutron detectors was placed, in a geometry identical to that described in [2]. They recorded the neutrons produced in the reaction in coincidence with the products detected in the telescope.

The first detector of the telescope provided a time signal that, together with the cyclotron radio frequency signal, produced the time of flight (TOF) value associated to each ion implanted in the telescope. A TOF vs. energy loss in the first detector (E1) spectrum indicated that the ^{10}Be impurity in the incident beam was below the 1% level. In the data reduction process, this impurity has been eliminated by adequate digital gates in TOF.

The main features of the method are presented in [1,4]. It is based on the fact that, for neutron halo nuclei, the breakup products have a narrow velocity distribution around the velocity of the projectile and that the emitted neutron, in most cases doesn't loose energy in the telescope. Therefore the energy deposited in the telescope when a ^{10}Be occurs is smaller than for a nonreacted ^{11}Be and a strong correlation is expected between the reaction energy and the two measurable quantities, the total deposited energy and the depth inside telescope where ^{10}Be stops: the smaller the reaction energy, the larger the total energy and the longer the path length. The path length is easily determined from the number of touched detectors (whose thicknesses are known) and the energy loss in the last detector. A careful examination of the correlation between the total energy deposit for the ^{11}Be breakup events and their

path length revealed the fact that these events split into two classes: one for which the correlation is as expected from an energy loss - range relation and another one for which this relation is broken. More precisely, for the last class of events, an energy excess appears in one of the touched detectors, the pattern of energy losses in the other detectors remaining practically unchanged. This higher energy deposit is due to the fact that, following the strong interaction of the halo neutron with the target nucleus, an extra energy is left in that particular detector where the reaction occurred, while ^{10}Be, nonaffected, continues traveling through the telescope, making appropriate energy losses. This observation allows a separation between the diffraction (and Coulomb) dissociation and absorption breakup events.

The cross sections for the two breakup mechanisms have been determined with two different methods. For the absorption breakup the extra energy tags the reaction detector, making possible to evaluate the integrated cross section value over the whole detector thickness. For diffraction dissociation breakup, because ^{10}Be and ^{11}Be have almost the same velocities and, therefore, the same stopping powers, the reaction detector could not be determined directly. Instead, a simple formula, as deduced in [1] can be written for the ^{11}Be energy at which the reaction occurred:

$$E_{reac} = \frac{E_{inc} - E_{tot}}{1 - q} \tag{1}$$

where q is the fraction of the ^{11}Be energy taken away by the ^{10}Be,E_{inc} is the incident energy and E_{tot} is the total energy deposited in the telescope. A good mean value of q would be 10/11, as the implied energies are much higher than the one neutron separation energy of ^{11}Be (504 keV) and therefore the ^{10}Be will have essentially the same velocity as ^{11}Be. The reaction energy of each detected ^{10}Be is thus calculated with the simple relation:

$$E_{reac}^{calc} = 11(E_{inc} - E_{tot}). \tag{2}$$

From the histogram of number of events vs. reaction energy the cross section can be determined as a function of energy:

$$\sigma_i = C\frac{N_i}{M\Delta x_i} \tag{3}$$

where N_i is the number of events in the bin i of reaction energy E_{reac}, Δx_i is the thickness of silicon that correspond to the energies defining the bin and M is the total number of particles traversing the detector. The resulted excitation function for the diffraction dissociation breakup is plotted in Fig. 1 (open circles).

Equations (1) and (2) show that the accuracy of the calculated reaction energy

depends not only on the resolution in total energy (FWHM=3.5 MeV) and incident energy ($\pm$0.6 MeV) but also on the distribution of q which originates in the momentum distribution of ^{10}Be resulting from breakup. One should note that, applying the above procedure on simulated samples of events, except for a region close to the incident energy, the excitation function used in the simulations is correctly retrieved over a large range of energies, even if, for a given particular event, the difference between the real and the calculated reaction energy (by applying the formula (1)) could be large (see [1] for details). If one would like to correctly reproduce the shape of the experimental excitation function around the incident energy where the effects of ^{10}Be momentum distribution are determinant, the simulations must include this distribution explicitly. Moreover, this observation permitted to deduce not only the width but also the shape of this distribution (see below).

For absorption breakup $E_{tot} > \Delta E_{11} + E_{10}$ and eq. (1) is no longer valid. However, in this case the reaction detector can be determined and the cross section is evaluated from eq. (3) where the index "i" stands now for the detector number. The obtained results are presented in Fig. 1 (full circles). The error bars are those resulting from statistics. However, the separation of the absorption events described above implies a somewhat arbitrary cut in the energy deposited in the reaction detector; this may lead to a depletion of absorption events in favor of diffraction whose upper limit is 5% of the diffraction cross section.

The continuous lines are calculations made with the Serber model as described in [2]. Both the trend with energy and the absolute values are surprisingly well described by these simple calculations. The present value for the total breakup cross section at 40 MeV/nucleon is consistent with the value deduced from the target-Z dependence observed by Anne et al. [2], but is about 150 mb below a previous measurement by Fukuda et al. [3].

As mentioned before, the method allowed for the determination of parallel momentum distribution of ^{10}Be resulting from breakup in the case of two mechanisms. If we denote by $\vec{p}$ the momentum of ^{10}Be after the reaction in the frame of ^{11}Be that initiated the reaction and by $\vec{p_0} = m_{10}\vec{p}_{11}^{\,lab}/m_{11}$, then the energy of ^{10}Be in the laboratory system is $E_{10}^{lab} = (\vec{p_0}^{\,2} + 2\vec{p_0}\vec{p} + \vec{p}^{\,2})/(2m_{10})$ For breakup reactions in the first detectors of the telescope, $p_0 \gg p$, and the variance of the E_{10}^{lab} distribution at a fixed reaction energy can be written, to a good approximation [4]:

$$\sigma^2_{E_{10}^{lab}} = \frac{\vec{p_0}^{\,2}\sigma^2_{p_z}}{m^2_{10}} \tag{4}$$

in which the z direction is taken along $\vec{p_0}$. Therefore, the energy distribution of E_{10} is determined by the distribution of p_0 (or, equivalently, reaction energies in the target detector) and by the parallel component of $\vec{p}$. The simulations

confirm that the effect of the perpendicular momentum distribution on the E_{10} energy distribution is negligible for all the reasonable values of the width of this distribution.

As mentioned above, the width of the q distribution is reflected by the shape of fall off in the excitation function of diffraction dissociation breakup toward the highest reaction energies (i.e. around the incident secondary beam energy). The relation between the variances of the q distribution and of the parallel momentum distribution is obtained by dividing eq. (4) by E_{reac}^2:

$$\sigma_q^2 = \frac{2\sigma_{p_z}^2}{m_{11}E_{reac}}. \tag{5}$$

Routinely, a lorentzian or a gaussian distribution is supposed for the parallel momentum distribution. However, such a distribution, though reflecting the decay pattern of a $2s_{1/2}$ w.f. which characterizes the halo neutron in ^{11}Be, completely ignores the effects of the reaction mechanism. Therefore we used the w.f. obtained by Nunes [5] in the particle - core excitation model to perform an extended Glauber calculation (as presented by Esbensen et al. [6]) of the momentum distribution of ^{10}Be resulting from diffraction and absorption. Due to the explicit inclusion of the reaction mechanism, these calculations were able to reproduce correctly the shape of the observed distribution of energies, without any artificial cuts in the momentum distributions. By varying the decay length of the asymptotic part of the w.f., one could obtain momentum distributions of different widths that have been subsequently used to produce simulated histograms. A χ^2 calculated between the experimental and simulated histograms served as a selection criterion.

In particular, a simulation with FWHM=0 MeV/c showed that the effects of detector resolution and incident energy distribution are small as compared to that of momentum distribution. For this breakup mechanism, the best agreement with the data has been obtained for a FWHM of 40±3 MeV/c (histogram in Fig. 1) where the error corresponds to a 10% increase of the χ^2.

The parallel momentum distribution of ^{10}Be produced in an absorption breakup reaction has been determined, as in [4], by observing the energies of ^{10}Be at the exit from the reaction detector. Such a spectrum is shown in Fig. 2 for the third detector. Besides the main peak, a tail is visibly extending toward lower energies. This tail can be qualitatively explained by the fact that collisions leading to absorption breakup may appear also at rather small impact parameters and then, the core may change its velocity to a smaller one as a result of a dissipative interaction with the target. These events, called in the following "background", though counted for evaluating the absorption breakup cross section, should be eliminated if one would like to determine the parallel momentum distribution of ^{10}Be as close to the one it had in the ^{11}Be. On the

other side, the lack of-information about the tail continuation under the peak makes the procedure of "background" subtraction somewhat arbitrary, with direct implications for the deduced width of the momentum distribution. Two procedures have been applied.

Firstly, simulations with various widths of the momentum distribution have been compared with the experimental distribution in Fig. 2 without any "background" subtraction but restricted to the central peak (without including the low energy tail). The simulations accounted for the effects due to the detector thickness, straggling and resolution. The contribution of these effects is shown in the figure by the dashed histogram in the simulation of which the momentum distribution is ignored. As in the case of dissociation breakup, a χ^2 test has been used to select the simulation best reproducing the data and to assign an error to the deduced width of parallel momentum distribution. The result was FWHM=46±3 MeV/c and this represents obviously an upper limit.

Secondly, the tail has been fitted with an exponential that extended up to the peak centroid, folded with the experimental resolution and the approximate momentum distribution as indicated in a first iteration by the central peak. The result is shown in the figure by the thin line. This "background" has been subtracted and the remaining distribution is represented in the inset. The histogram is the result of a simulation in which the longitudinal momentum has a FWHM=40±3 MeV/c and it represents the best fit to the data.

It is important to observe that the inclusion of the reaction mechanism effects spared the need of any artificial cuts in the momentum distribution, the tail of the distribution at high energies being straightforwardly reproduced. Similar values have been obtained for all the first four detectors, showing no significant energy dependence for the scanned region (25–40 MeV/nucleon). The energies at which the parallel momentum distribution have been measured are obviously the same as the values in Fig. 1 at which the absorption breakup cross sections have been given. The different values of the widths found for dissociation and absorption breakup, when weighted with the corresponding cross section values yield a mean value which is in fair agreement with the FWHM=43.6±1.1 MeV/c measured by Kelly et al. [7] in an experiment that has not distinguished the two mechanisms.

One should mention that some events in the "background" may have a different nature: the ^{10}Be core may have had a close interaction with the target as a result of which it has lost some of its kinetic energy (and an extra energy has been deposited in the reaction detector) while the halo neutron detached itself from the core and continued to move in the forward direction. Obviously, this is not an absorption event but neither it is a diffraction one in the sense of the definition given at the beginning of this paper. Our data show a rate of neutron coincidences which is ten times higher in the case of diffraction than in

the case of absorption. This fact supports the performed assignment of events to absorption and diffraction. Moreover, in the case of absorption, the coincidences appear essentially with "background" events, being almost completely absent under the peak in Fig. 2. The angular distribution of these neutrons is forwardly peaked and they have high energies. All these facts indicate that, in the case of absorption, most coincident neutrons come from "background" events having the nature mentioned at the beginning of the paragraph.

A procedure similar to the one described above for the one neutron breakup has been applied for the two neutron breakup cross section: ^{11}Be$\rightarrow^{9}$Be+n+n. In this case the eq.(1) must take into account the binding energy of the two neutrons $E_{reac} = (E_{inc} - E_{tot} - qS_{2n})/(1-q)$ where the mean q value is now 9/11 and S_{2n}=7.32 MeV. Of course, in this case the distribution in q is much broader and the reaction products, especially at low reaction energies will be no longer very forwardly focused. That will lead to an important number of escapes from the telescope. Fig. 3 shows the obtained results. The shape of the dissociation breakup excitation function is qualitatively reproduced when a large FWHM is set in simulation for the q distribution and a value of 12±4 mb can be extracted for the cross section at the highest reaction energies. The plotted error bars for the absorption component represent only the statistical error. An additional error of ±3 mb due to ^{10}Be contamination and to escapes has been estimated. One should note the differences compared to one neutron breakup: the absorption component is in this case almost three times larger than the dissociation one and their sum amounts to about one tenth of the one neutron breakup cross section.

The detecting device allowed the determination of charge changing cross sections for both ^{11}Be and ^{10}Be (the last one was the impurity in the secondary beam). The method is presented in [4] and details will be given in a forthcoming publication.

The results are plotted in Fig. 4. Though the error bars are rather large, the two cross section values are close to each other. This supports the assumption that the densities of the protons are similar for the two nuclei and that the halo neutron does not affect the structure of the core (^{10}Be).

Furthermore, the total reaction cross of ^{11}Be on silicon, σ_R^{11} can be evaluated from $\sigma_R^{11} = \sigma_{CC}^{11} + \sigma_{inel}^{11} + \sigma_{-n}^{11} + \sigma_{-2n}^{11}$. With a calculated inelastic cross section of 80mb (60mb for ^{11}Be excitation and 20mb for silicon excitation), the result is 2.15±0.07 b at 30 MeV/nucleon incident energy. Fukuda et al.[3], reported a reaction cross section value of 2.27±0.05 b at 33 MeV/nucleon for an ^{27}Al target but the disagreement may be due to the larger breakup cross section (650^{+250}_{-50} mb) they have obtained. In this respect one should mention that our calculations for the reaction cross section using the Glauber model are in agreement with the value we found. Similarly, $\sigma_R^{10} = \sigma_{CC}^{10} + \sigma_{inel}^{10} + \sigma_{-n}^{10}$.

In the approximation $\sigma^{10}_{-n}=\sigma^{11}_{-2n}$ and with an estimated inelastic cross section of 30mb one obtains for $\sigma^{10}_{R}=$ 1500±70mb at 40 MeV/nucleon, again well reproduced by a Glauber calculation. The value recently reported by Warner et al. [8] for the reaction cross section of ^{10}Be on silicon (an interpolation suggests 1.55±0.05 b at 45 MeV/nucleon) is in agreement with our value.

In conclusion, the separate contributions of diffraction and absorption to the breakup cross section have been determined; they are well reproduced by Serber type calculations. The parallel momentum distributions for the ^{10}Be have been determined in the two cases. Detailed microscopical calculations showed the importance of the reaction mechanism on the observed distributions. Charge changing cross sections have been measured for ^{11}Be and ^{10}Be as well as two neutron breakup cross section for ^{11}Be (for diffraction and absorption). All the mentioned data, taken in a single experiment, provide new important information about the structure and breakup mechanism of the halo nucleus ^{11}Be in the energy range 20−40 MeV/nucleon, that severely constrains the theoretical interpretations.

References

[1] J.M.Corre et al., NIM A359(1995)511.

[2] R.Anne et al., Nucl. Phys. A575(1994)125.

[3] Fukuda et al., Phys. Lett. B268(1991)339.

[4] F. Negoita et al., Phys. Rev. C 54(1996)1787.

[5] F. M. Nunes, I. J. Thompson and R. C. Johnson, Nucl. Phys. A596(1996)171; F. M. Nunes, J. A. Christley, I. J. Thompson and R. C. Johnson, Nucl. Phys. A609(1996)43.

[6] H. Esbensen in Extremes of Nucl. Structure, Proc. Int. Workshop XXIV, Hirchegg, Austria, Jan. 15-20 1996, ed. by H. Feldmeyer, J. Knoll and W. Norenberg.

[7] Kelly et al., Phys. Rev. Lett. 74(1995)30.

[8] Warner et al., Phys. Rev. C 54(1996)1700.

Figure captions

Fig. 1. The experimental values of diffraction dissociation breakup (open circles), absorption breakup (full circles) and total breakup (squares) cross sections as a function of reaction energy. All cross sections refer to one neutron breakup. The histogram is the result of a simulation including a parallel momentum distribution of ^{10}Be with FWHM=40 MeV/c. The curves represent calculations within the Serber model described in [2]. See text for details.

Fig. 2. Absorption breakup events in the third detector have been selected. The energy of ^{10}Be at the exit of target detector, E_{10}, is determined by summing up the energies deposited in all subsequent detectors. The FWHM of the experimental spectrum (points) is reproduced (thick line histogram) when the width of parallel momentum of ^{10}Be in the rest frame of ^{11}Be is 46 MeV/c. Dashed line histogram is a simulation with FWHM=0 MeV/c. In the inset is presented the "background" subtracted spectrum and a simulated histogram with FWHM=40 MeV/c.

Fig. 3. The points correspond to experimental cross section for the absorption component of the two neutron breakup. The histogram is the obtained excitation function for diffraction dissociation two neutron breakup, strongly distorted by the large momentum distribution of ^{9}Be (see text).

Fig. 4. Experimental charge changing cross section for ^{11}Be (open circles) and ^{10}Be (full circles).

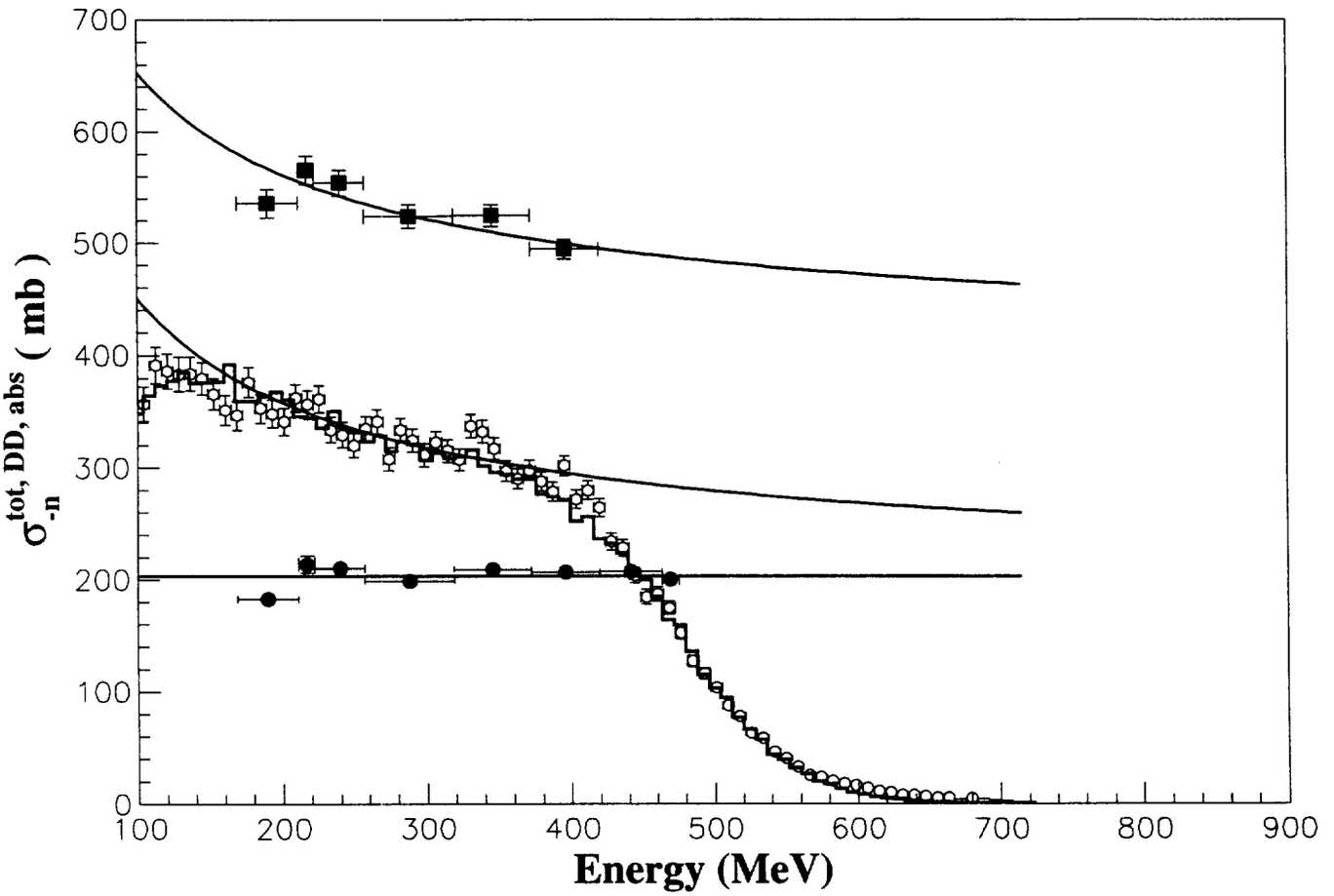
700
600
500
400
300
200
100
0
100
200
300
400
500
600
700
800
900
$\sigma^{tot, DD, abs}_{-n}$ (mb)
Energy (MeV)

Fig. 1

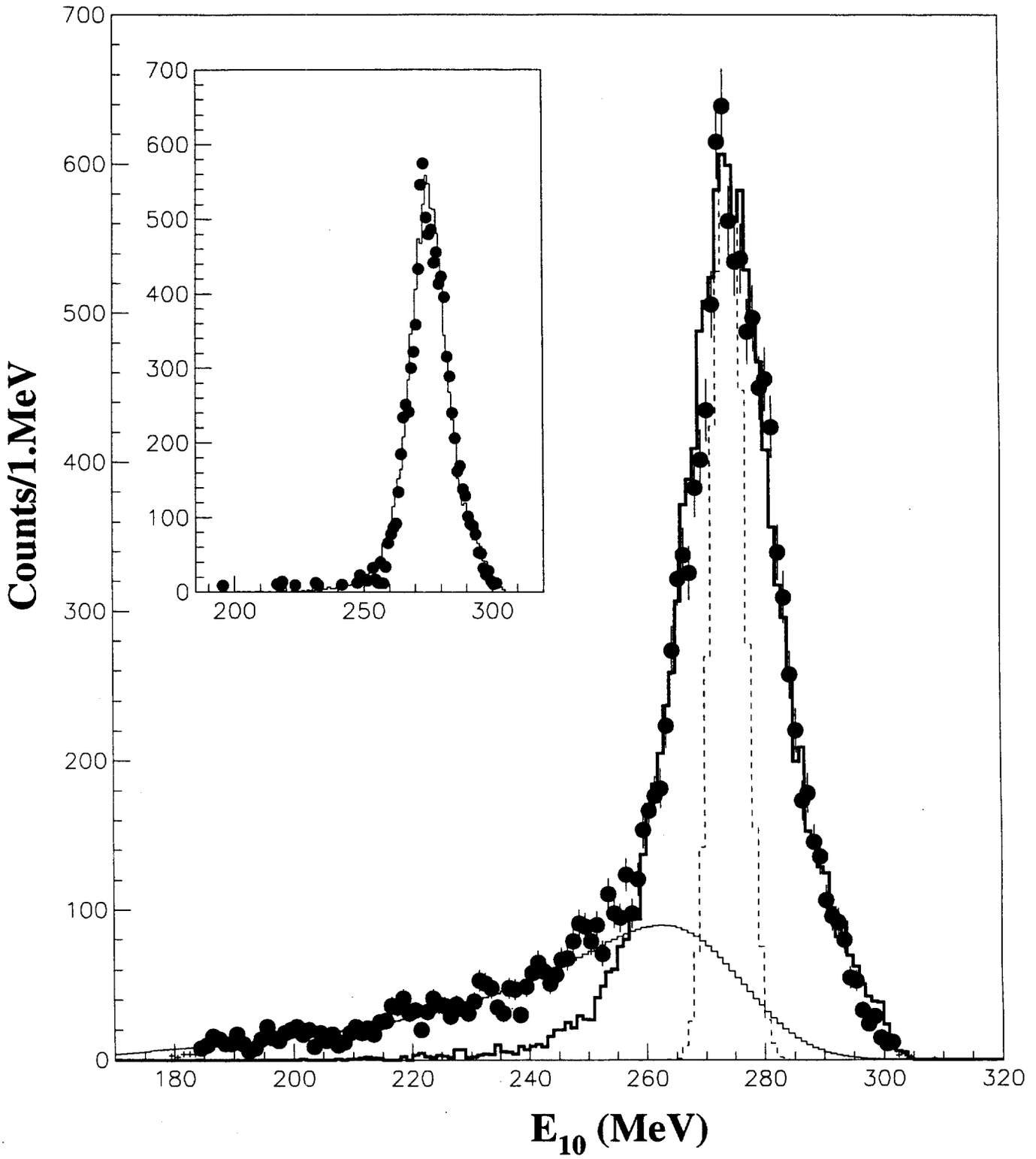
Counts/1.MeV
E_{10} (MeV)
0
100
200
300
400
500
600
700
180
200
220
240
260
280
300
320
0
100
200
300
400
500
600
700
200
250
300

Fig. 2

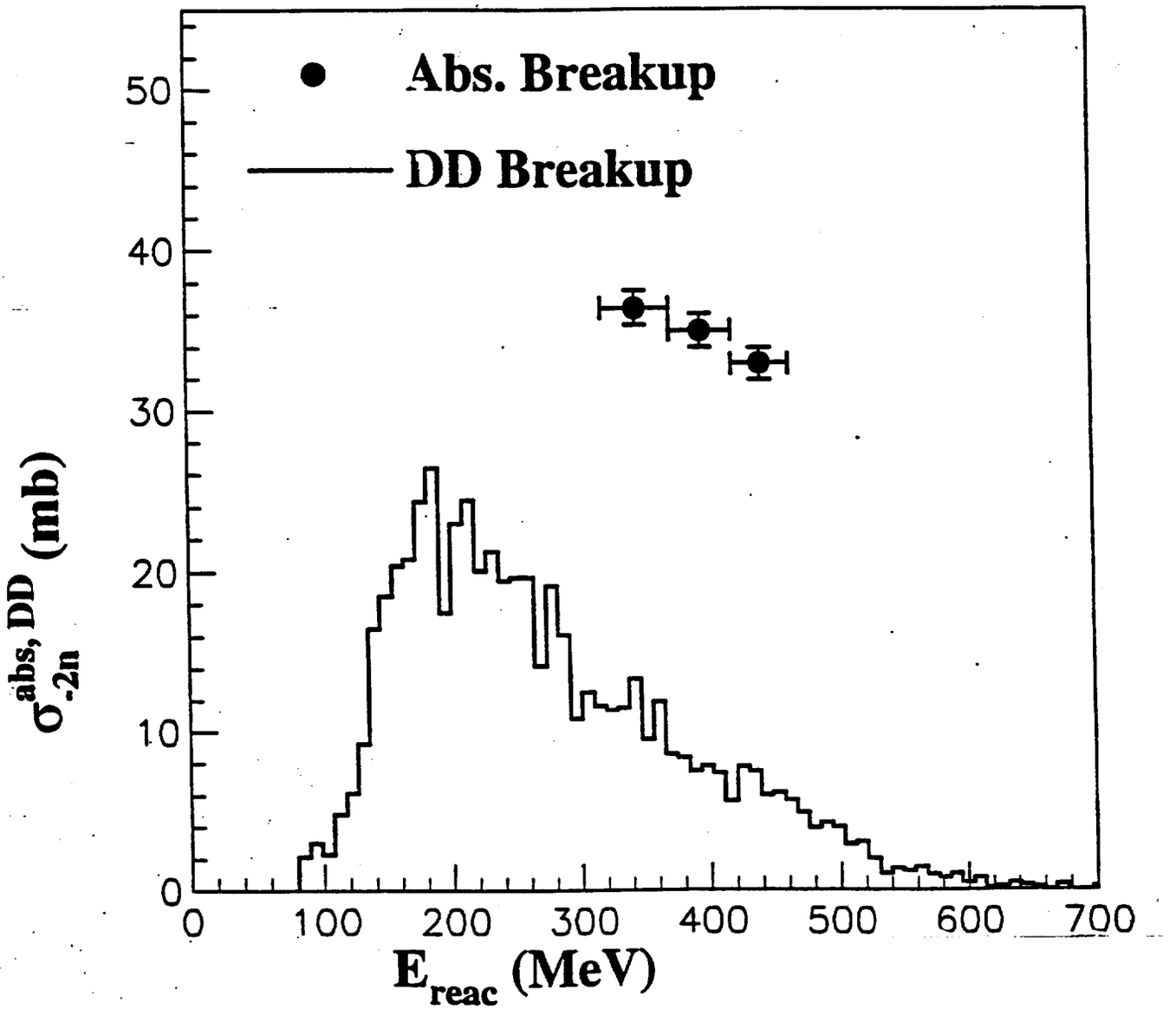
Abs. Breakup
DD Breakup
$\sigma_{-2n}^{abs,\ DD}$ (mb)
E_{reac} (MeV)
0
10
20
30
40
50
0
100
200
300
400
500
600
700

Fig. 3

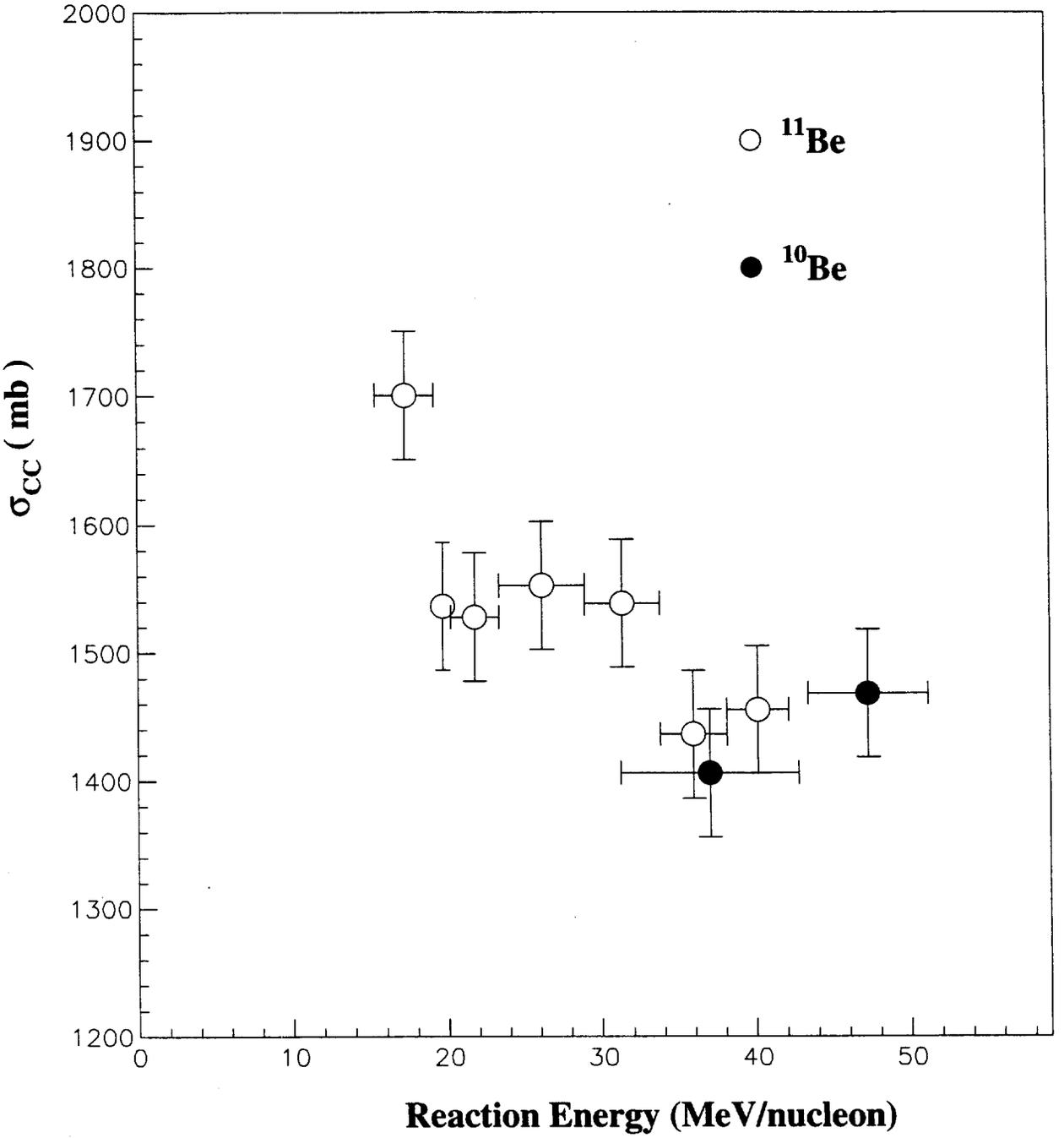
2000
1900
1800
1700
1600
1500
1400
1300
1200
0
10
20
30
40
50
σ_{CC} (mb)
Reaction Energy (MeV/nucleon)
^{11}Be
^{10}Be

Fig. 4